Schematic Eye Models for Simulation of Patient Visual Performance

James B. Doshi, MD; Edwin J. Sarver, PhD; Raymond A. Applegate, OD, PhD

ABSTRACT

PURPOSE: To determine if model eyes can simulate the visual performance of normal human eyes under conditions of varying low myopic blur, pupil size, and contrast.

METHODS: High and low contrast Bailey-Lovie logMAR visual acuity (VA) of three normal eyes of three subjects were measured for four artificial pupil sizes and ten levels of myopic defocus. Simulated visual acuities were then determined for three model eyes—the Indiana Eye with no spherical aberration, the Indiana Eye with average spherical aberration, and the Kooijman Eye—by generating optically aberrated VA charts for each testing condition using Visual Optics Lab software by Sarver and Associates, Inc, and having the subjects read high resolution printouts of these charts using a 3-mm pupil and optimal spectacle correction. The correlation between real VA and simulated VA was then plotted and a regression line calculated.

RESULTS: Slopes for the Indiana Eye, Indiana Eye with spherical aberration, and Kooijman Eye were 0.98, 0.98, and 1.01 for high contrast, and 0.92, 0.67, and 0.75 for low contrast, respectively. The r^2 values were 0.73, 0.74, and 0.77, for high contrast, and 0.69, 0.40, and 0.50 for low contrast, respectively. Under low contrast conditions the Indiana Eye VA was significantly closer to the real VA than that of the other two models ($P<.0003$).

CONCLUSION: Visual performance can be simulated by eye models. The simple single surface Indiana Eye with no spherical aberration best modeled both high and low contrast visual acuity. [*J Refract Surg* 2001;17:414-419]

Schematic eye models can be used to model the optical properties of normal and pathologic eyes, and to develop and evaluate optical corrections designed to improve retinal image quality. Such corrections include spectacles, contact lenses, intraocular lenses, and refractive surgery.

Early eye models with some degree of optical and anatomic accuracy were developed almost a century ago by Gullstrand[1] and Von Helmholtz.[2] Their models used data from clinical measurements and employed spherical surfaces for the cornea and lens to predict first order optical properties. More recently, models have been used to simulate optical functions such as control of retinal illumination[3], chromatic aberration[4], and retinal image formation.[5] The Kooijman model employed aspheric surfaces for the cornea, lens, and retina and was used to study retinal illumination.[3] The Indiana eye was developed to model the chromatic aberration of the eye.[4] More recently, Camp and colleagues used corneal first surface topography data to form a single refracting surface to model the optical imaging properties of the corneal first surface.[5,6] In their study, corneal topography data from patients with keratoconus, radial keratotomy, and epikeratoplasty were used to generate simulated retinal images formed by the corneal first surface of Snellen letters. Their study showed that different corneal shapes produced different point spread functions causing variations in image quality that could be easily perceived subjectively in the Snellen letter images. Grievencamp and colleagues[7], expanding on this work, used the Kooijman model and exact raytracing to produce simulated retinal images of Snellen "E"s. In their study, they included the effects of both diffraction and retinal directionality, and generated

From the Department of Ophthalmology, University of Texas Health Science Center at San Antonio, San Antonio, TX (Doshi, Applegate), and Sarver and Associates, Inc., Merritt Island, FL (Sarver).

Edwin J. Sarver and Raymond A. Applegate have proprietary interests in VOL-3D.

This work was funded by NIH grant R01 EY-08520 to RAA and R44 EY11681 to EJS, an unrestricted research grant to the Department of Ophthalmology, University of Texas Health Science Center at San Antonio, San Antonio, Texas and by Research to Prevent Blindness, New York, NY.

The authors thank Gene Hilmantel for his assistance with the statistical analysis.

Correspondence: Raymond A. Applegate, OD, PhD, Department of Ophthalmology, University of Texas Health Science Center at San Antonio, San Antonio, TX 78284-6230. Tel: 210.567.8429; Fax: 210.567.8413; E-mail: applegate@uthscsa.edu

Received: October 20, 2000

Accepted: March 21, 2001

images under conditions of simulated blur from 0 to 5.00 diopters (D) for pupil diameters between 0.5 to 7 mm. Predicted visual acuity was determined by calculation. They determined the smallest "E" that a normal individual should be able to identify given an average contrast sensitivity function. Their work revealed modeling had excellent promise for predicting actual visual performance of individual patients by showing a high correlation between their predicted visual acuity and published clinical data for similar levels of blur ($r^2 = 0.909$).

In the present study the authors utilized eye models of varying complexity to determine if they could in fact "see" like a human eye. To this end, we generated hard copies of the models' retinal images projected into object space for different blur levels, pupil size, and contrast level (high and low contrast logMAR charts) and asked optimally corrected subjects to read the resulting charts through a 3-mm pupil. We then determined the coefficient of correlation between simulated visual acuity and actual visual acuity for the same test conditions.

SUBJECTS AND METHODS

Overview of Two Experiments

In the first experiment, each subject's high and low contrast acuity was measured for a variety of levels of myopic blur and pupil sizes. In the second experiment, using each of three different model eyes, the retinal images of Experiment One were simulated, projected into object space, and printed using a high-resolution printer. Simulated visual acuity was determined by optimally correcting each subject and measuring the visual acuity to each retinal image simulation through a 3-mm pupil. The acuities of Experiment Two were then plotted against the acuities of Experiment One to determine how well the simulated charts mimicked actual acuity.

Subjects

All subjects gave written informed consent for the experiment.

Three individuals with no known ocular or systemic abnormalities and best spectacle-corrected visual acuity of 20/15 or better served as subjects. The cycloplegic spherical equivalent refractions were: subject 1 (age 50) right eye, -5.50 +2.25 x 125°; subject 2 (age 27) left eye, -3.25 +1.25 x 127°; and subject 3 (age 26) left eye, plano.

Table 1
Parameters of the Kooijman Eye Model

	Corneal Anterior Surface	Corneal Posterior Surface	Lens Anterior Surface	Lens Posterior Surface	Retina
Radius (mm)	7.8	6.5	10.2	-6.0	-14.1
Shape factor (p)	0.75	0.75	-2.06	0.01	---
Distance from anterior pole (mm)	0.0	0.55	3.6	7.6	24.2
Index of refraction	1.3771 (cornea)	1.3374 (aqueous)	1.42 (lens)	1.336 (vitreous)	---

Experimental Conditions

Ten different myopic defocus lenses (0.00, 0.125, 0.25, 0.375, 0.50, 0.75, 1.00, 2.00, 3.00, and 4.00 D), four different artificial pupil sizes (2, 4, 6, 8 mm), and two contrast levels of acuity charts (Bailey-Lovie high contrast and low contrast) were used for a total of 80 experimental conditions for each subject in each experiment. The Indiana Eye (IE), developed by Larry Thibos and Arthur Bradley, is a single surface model in which axial length = 22.22 mm, n = 1.333, with an aspheric "corneal" surface, with an apical radius of r = 5.55 mm and a shape factor p = 0.4375. The Indiana Eye with spherical aberration (IEwSA) model is the Indiana Eye modified to have an average amount of spherical aberration. Parameters are the same as the previous model except the corneal shape factor is p = 0.6 (ellipsoid). The Kooijman Eye (KE) has four refracting surfaces, defined in Table 1.

Testing Protocol

After signing an informed consent and receiving an explanation of the testing procedures, each subject was cyclopleged with 1% tropicamide hydrochloride and phenylephrine 2.5% drops instilled every 90 minutes during testing. Testing did not begin until each subject's test eye had dilated to at least 8 mm. Each subject was grossly aligned to a trial frame fixed in space using a bite bar mounted to a three-dimensional vise (positioning accuracy, ±.01 mm). Gross alignment to the trial frame was complete when a visual acuity chart appeared centered in the field of view through a 1-mm pinhole mounted in the rear slot of the trial frame. The vertex distance (z alignment) was refined by replacing the pinhole with an "eye poker" (a rounded 13-mm narrow post that locked into the back most cell of the trial frame). The subject was slowly advanced

with their eye closed using the compound vise until the eyelid just touched the end of the eye poker. The eye poker was then removed and replaced with a 1-mm artificial pupil. Final x-y alignment was achieved using a foveal achromatic alignicator[8-10] to align the artificial pupil to the foveal achromatic axis. On the assumption that the eyelid is approximately 1 mm thick, the vertex alignment placed each component contained in the trial frame at the following vertex distances: artificial pupil, 14 mm; spectacle, 19 mm; spectacle cylinder, 22.5 mm; blurring lens, 26 mm.

Subject Visual Acuity

Visual acuity of the three subjects was measured for ten different blur levels, four different pupil sizes, and two contrast levels (10% low contrast and high contrast) using Bailey-Lovie logMAR visual acuity charts. Chart illumination was 160 ft Lamberts. Three high contrast and three low contrast charts each with different randomized letters were used. The charts were scaled for a 1.22-m testing distance and printed on photo quality glossy 8.5 x 11-in paper allowing for a range of logMAR visual acuity (VA) between -0.3 and 1.0. The subject read the chart until five letters were misread. As higher power defocusing lenses were used, the subject was forced to read a different part of the chart, reducing issues of memorization. The logMAR VA was calculated to the letter by assigning each correct letter a value of 0.02 log units. The subject was refracted each time the artificial pupil was changed in order to give optimal baseline acuity for the 1.22-m testing distance.

Model Visual Acuity

To determine the visual performance of the models, simulated retinal images for each pupil size, blur level, and model eye were generated in object space for a 1.22-m viewing distance using Visual Optics Lab-3D (VOL-3D) software (Sarver and Associates, Inc., Merritt Island, FL). VOL-3D software uses a fast discrete Fourier transform of the object intensity array and point spread function to find the object intensity spectrum and optical transfer function. The image intensity spectrum and image intensity array were then calculated and converted to a simulated image that was printed on the same Epson Photo Quality printer and paper used to create the perfectly imaged test charts used in experiment one. A blurred chart was thus created for each testing condition for each eye model. In Figure 1, we present four charts reduced in size to accommodate journal format. The upper left chart is a retinal image projected into object space of a diffraction limited high contrast logMAR chart for a 6-mm pupil. The upper right chart is a retinal image projected into object space of a diffraction limited low contrast logMAR chart for a 6-mm pupil. The lower two charts are corresponding charts in the presence of 0.50 D of myopic blur. Figure 2 illustrates the effect of pupil size in the presence of 0.50 D of myopic blur.

The model's visual acuity was measured by having the cyclopleged subjects read the 80 blurred charts using their optimal spectacle correction and a 3-mm artificial pupil. Presentation order was randomized. It is recognized that human eyes have their own aberrations that will interact with the blurred charts and affect the measured VA. The effect of naturally occurring aberrations were minimized by using normal eyes with optimal spectacle correction and a 3-mm artificial pupil.

Test-retest Reliability

The test-retest reliability was determined by testing each subject twice for all conditions of experiment one and plotting re-test VA against test VA for each condition. For the high contrast acuity condition, the coefficient of determination (r^2) for test-retest was 0.93 and the slope of the regression was 1.03 with a y-intercept of -0.042. For the low contrast acuity condition, the coefficient of correlation for test-retest was 0.84 and the slope of the regression was 0.921 with a y-intercept of -0.064.

RESULTS

The correlation between model VA and subject VA was determined for each model by plotting model VA vs. subject VA for each subject. Data for the subjects were pooled and a regression line calculated. If the model eye perfectly simulated the subject's visual performance, then the line would have a slope of 1.00, a y-intercept of 0.00, and an r^2 of 1.00.

Figure 3 shows the correlation between the Kooijman Eye simulated visual acuity and the actual visual acuity of the three subjects. For this particular model eye, the slope for the best fitting line is 1.01, and the r^2 is 0.77. The slopes and the coefficients of correlation for all three models are displayed in Table 2 for both high and low contrast acuity conditions.

As can be seen in Table 2, for the high contrast condition all three model eyes performed similarly. For all the models the correlation between simulated high contrast acuity and actual high contrast

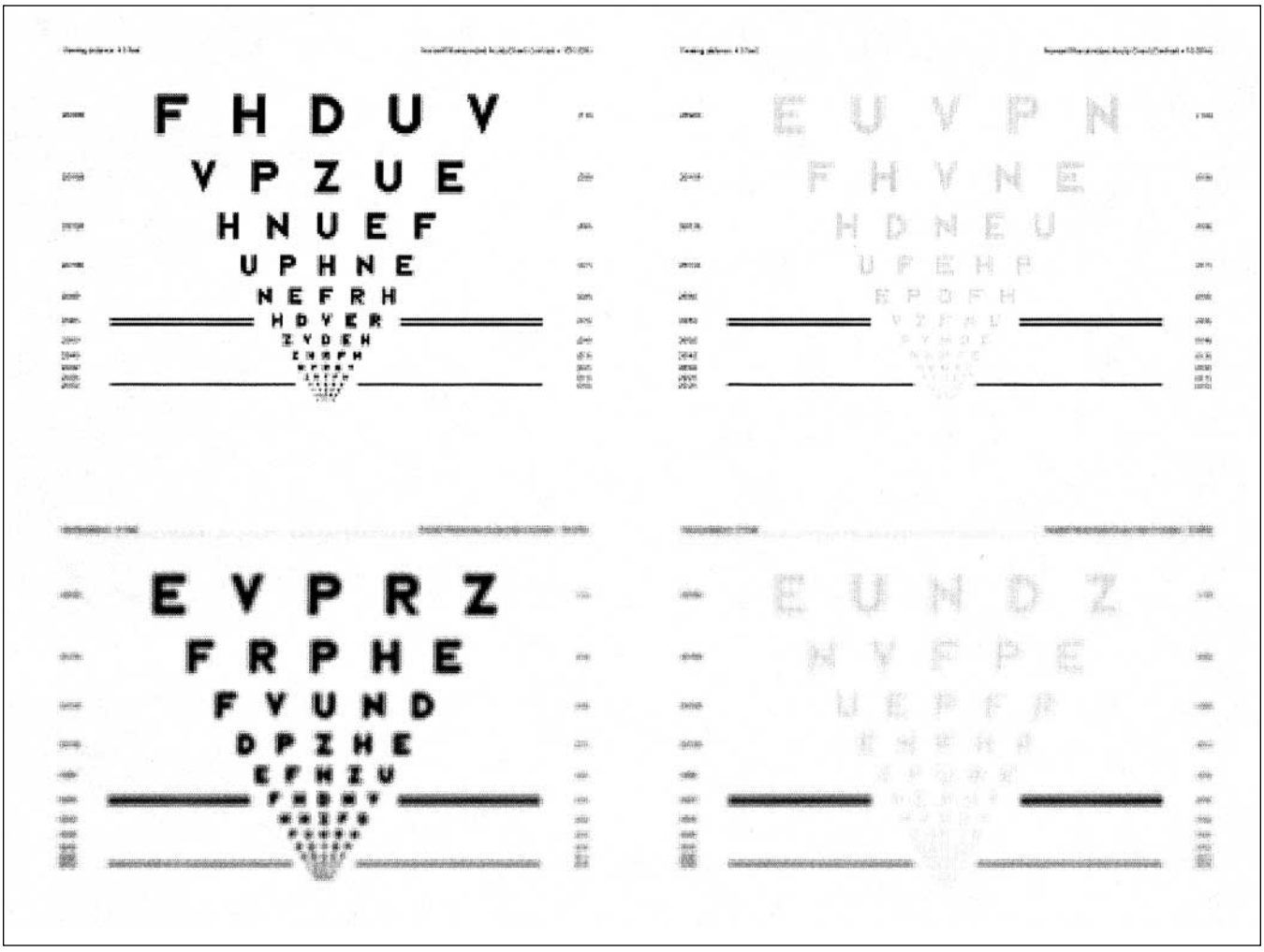

Figure 1. The charts are retinal images projected into object space of a diffraction limited high (left panel) and low (right panel) contrast logMAR chart for a 6-mm pupil. The lower charts are the same charts as above except in the presence of 0.50 D of myopic blur. Viewing distance 41 cm (16 inches).

acuity had slopes very close to 1.00 and high r^2 values, albeit slightly lower than the r^2 for the test-retest correlation. Under low contrast the Indiana Eye, the simplest of the models, had the slope closest to 1 and the highest r^2. To compare the models with each other the mean absolute difference between the model VA and subject VA for all testing conditions was determined for each model. Analysis of variance was used to identify significant differences. For high contrast conditions, no significant difference between the models was found. However, for low contrast, the Indiana Eye simulated VA was significantly closer to the actual subject VA than for either the Indiana Eye with spherical aberration ($P<.0001$) or the Kooijman Eye ($P<.0003$), as determined by the Fisher's protected least significant difference test.

Table 2
Slope and Coefficient of Correlation (r) for the Linear Regression Between Simulated Acuity and Actual Acuity for Three Eye Models

	Indiana Eye	Indiana Eye With Spherical Aberration	Kooijman Eye
High Contrast Acuity			
Slope	0.98	0.98	1.01
r^2	0.73	0.74	0.77
Low Contrast Acuity			
Slope	0.92	0.67	0.75
r^2	0.69	0.40	0.50

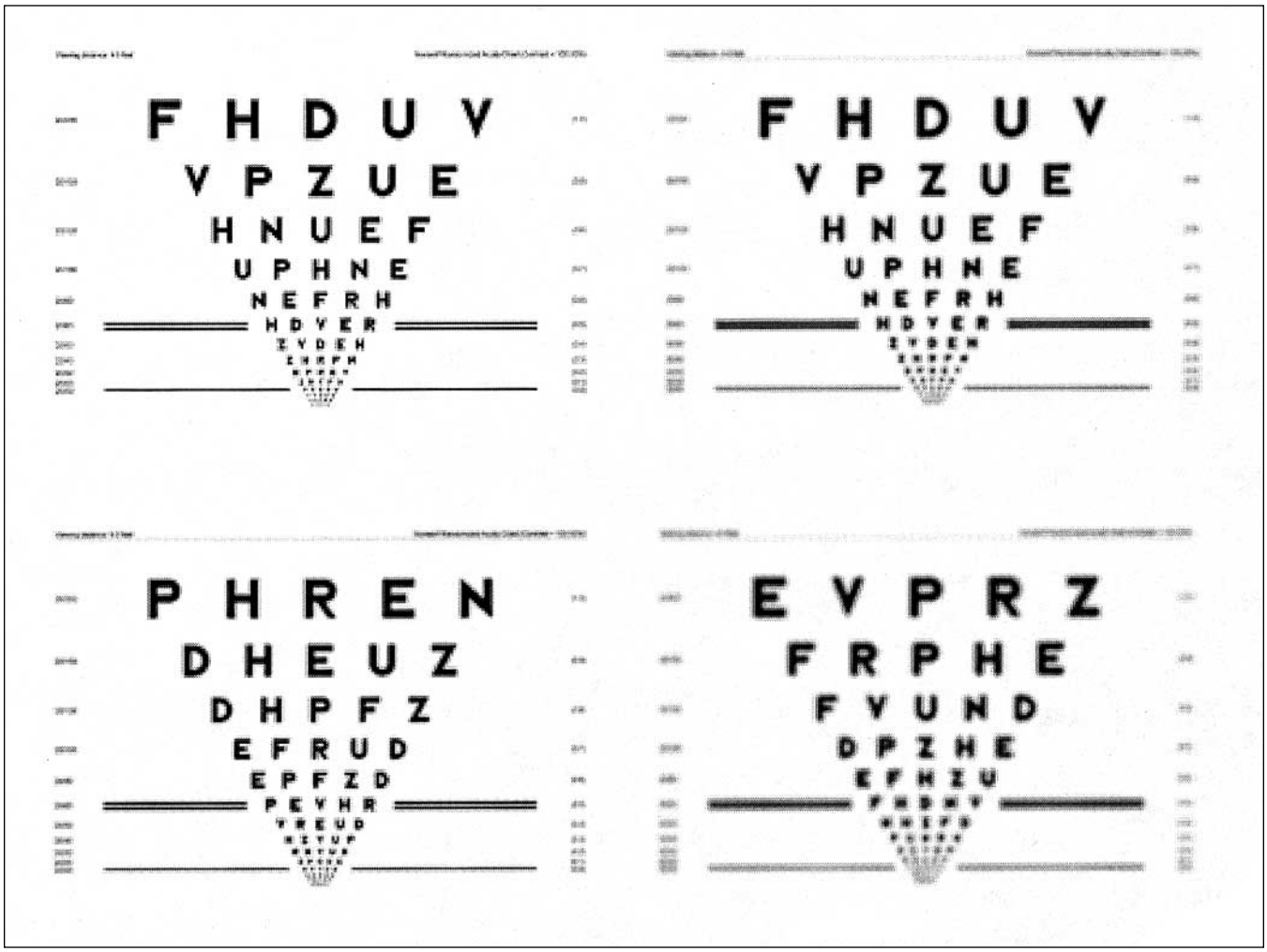

Figure 2. The effect of pupil size in the presence of 0.50 D of myopic blur on retinal images projected into object space. **Upper left panel)** Appearance of the chart without blur; **Lower left panel)** 0.50 D myopic blur through a 2-mm pupil. **Upper right panel)** 0.50 D myopic blur through a 4-mm pupil. **Lower right panel)** 0.50 D myopic blur through a 6-mm pupil. Viewing distance 41 cm (16 inches).

DISCUSSION

Three eye models were employed to simulate the retinal images and, in turn, the visual performance as measured by high and low contrast visual acuity of optically aberrated eyes. A high correlation was found between the simulated VA and the actual VA. The r^2 in the high contrast condition was 0.73, or slightly better, depending on the particular model with no significant differences between the three models. That is, 73% or more of the variance in actual VA can be accounted for by the variance in the simulated VA. Given that the r^2 for test-retest for high contrast acuity is 0.93, these simple models performed well, albeit not perfectly. The lack of significant differences between models in the high contrast condition indicate that the addition of average spherical aberration in the Indiana Eye or multiple refracting surfaces in the Kooijman Eye provides no improvement in high contrast retinal image quality over the simple Indiana Eye.

Under the more difficult low contrast conditions, the single surface Indiana Eye performed significantly better than either the Indiana Eye with spherical aberration or the Kooijman Eye. Here, the addition of average spherical aberration found in the Indiana Eye with spherical aberration significantly decreased the visual performance of the model, as did adding multiple surfaces, as in the Kooijman Eye model.

It may be possible to improve the ability of model eyes to mimic an individual's actual visual performance by including the actual ocular aberrations of the individual's eye into the model. Such an approach could be accomplished by measuring the optical aberrations of the eye (eg, using the now commercially available Shack/Hartmann sensor)

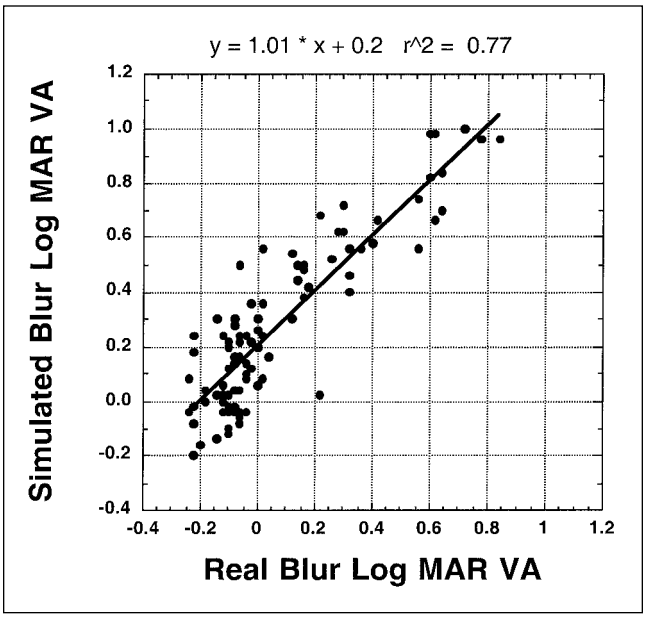

Figure 3. Plot of model visual acuity vs. subject visual acuity for the Kooijman Eye model under high contrast conditions. Data are pooled for all subjects, pupil sizes, and levels of defocus.

and incorporating the measured aberrations into a simple single surface model.

Given that the current models simulated true visual acuity performance well, and that in all likelihood future models will do even better, such models can be used to develop, improve, and/or optimize refractive therapy prior to human subject testing. This would reduce the time and cost to bring new therapy to the market. Perhaps most importantly, models could be used to display how a particular individual sees. Such a process would be useful to family members, caregivers, and society to better understand the needs of patients with significant aberrations of the eye's optics. In the same vein, simulated retinal images could be used to illustrate the range of likely outcomes of various refractive procedures prior to surgery, as part of the informed consent.

REFERENCES

1. Gullstrand A. Appendices to part I. In: von Helmholtz H. Physiologic Pptics, 3rd ed. Volume 1. Hamburg, Germany: Voss; 1909:350-358.
2. von Helmholtz H. Physiologic Optics, 3rd ed. Volumes 1 and 2. Hamburg, Germany: Voss; 1909:91-121.
3. Kooijman AC. Light distribution on the retina of a wide-angle theoretical eye. J Opt Soc Am 1983;73:1544-1550.
4. Thibos LN, Bradley A. Modeling the refractive and neurosensor systems of the eye. In: Indiana University Cognitive Science Program. Bloomington, IN; 1997:8.
5. Camp JJ, Maguire LJ, Cameron BM, Robb RA. A computer model for the evaluation of the effect of corneal topography on optical performance. Am J Ophthalmol 1990;109: 379-386.
6. Camp JJ, Maguire LJ, Cameron BM, Robb RA. An efficient ray tracing algorithm for modeling visual performance from corneal topography. In: Proceedings of the First Conference on Visualization in Biomedical Computing, Atlanta, GA, May 22-25. Piscataway, NJ: IEEE; 1990.
7. Grievenkamp JE, Schwielgerling J, Miller JM, Mellinger MD. Visual acuity modeling using optical raytracing of schematic eyes. Am J Ophthalmol 1995;120:227-240.
8. Thibos LN, Bradley A, Still DL, Zhang X, Howarth PA. Theory and measurement of ocular chromatic aberration. Vision Res 1990;30:33-49.
9. Simonet P, Campbell MCW. The optical transverse chromatic aberration on the fovea of the human eye. Vision Res 1990;30:187-206.
10. Rynders M, Lidkea B, Chisolm W, Thibos LN. Statistical distribution of foveal transverse chromatic aberration, pupil centration, and angle psi in a population of young adult eyes. J Opt Soc Am A 1995;12:2348-2357.